

Microscopic origin of molecule excitation via inelastic electron scattering in scanning tunneling microscope

Guohui Dong,¹ Yining You,² and Hui Dong^{1,*}

¹Graduate School of Chinese Academy of Engineering Physics, Beijing 100084, China

²Department of Modern Physics, University of Science and Technology of China, Hefei 230026, China

The scanning-tunneling-microscope-induced luminescence emerges recently as an incisive tool to measure the molecular properties down to the single-molecule level. The rapid experimental progress is far ahead of the theoretical effort to understand the observed phenomena. Such incompetence leads to a significant difficulty in quantitatively assigning the observed feature of the fluorescence spectrum to the structure and dynamics of a single molecule. This letter is devoted to reveal the microscopic origin of the molecular excitation via inelastic scattering of the tunneling electrons in scanning tunneling microscope. The current theory explains the observed large photon counting asymmetry between the molecular luminescence intensity at positive and negative bias voltage.

Introduction – The physical limitation of conventional semiconductor devices spurs the recent development of single molecule photoelectronics [1–3], where the incisive tool to probe single molecular structure and dynamics is of great demand. Combining the high resolution of scattering tunneling microscope (STM) with the specificity of fluorescence spectroscopy of molecules, STM-induced luminescence (STML) provides an ideal tool to study the photon emission and dynamics on the single-molecule level [4, 5]. Experimental breakthroughs have allowed direct observations of the single-molecular properties, e.g., the dipole-dipole coupling between molecules [6–8], the energy transfer in molecular dimers [9], and the Fano-like lineshape [10–12]. Yet, the retarded theoretical followup prevents us from conclusively understanding the single-molecular properties through the quantitative analyses of experimental data.

Such lag of the corresponding theoretical effort has led to inconsistent between experimental explanations. The underlying origin of the asymmetric emission intensity at positive and negative bias between the tip and substrate was assigned as the carrier-injection mechanism in [6], while it was also understood as inelastic electron tunneling (probably mediated by the localized surface plasmon) [13] for the same molecule, i.e., the single ZnPc molecule. The question exists even on the asymmetry with larger tunneling current at positive bias or versa [6, 13]. The inconsistency remains unresolved mainly due to the lack of microscopic theory to conclusively determine the properties of the different tunneling mechanisms, which are mixed in the *ab initio* calculations [14, 15].

In this letter, we reveal the underlying microscopic origin of the inelastic electron scattering down to the basic Coulomb interaction between the tunneling electron and the single molecule. Our theory shows the asymmetry with larger tunneling current and photon counting rate at negative bias, in turn, excludes the possibility of the opposite asymmetry to be attributed to the inelastic electron scattering. Such attempt shall initiate the understanding of the experimental feature from its microscopic origin and stimulate the theoretical studies of the STML.

Model – For the clarity of the notation, we sketch the design

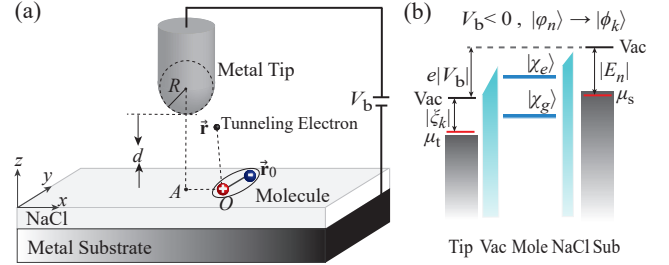


Figure 1. (Color online) (a) Schematic diagram of STML of a single molecule placed on a salt-covered metal plane. The STM tip apex is modeled as a sphere with radius R . Point A is the projection of tip's center on the plane, and d is the distance between tip and plane. The position of the positive charge in the molecule (red) is set as the origin of the coordinate system. \vec{r} and \vec{r}_0 stand for the vector of the tunneling electron (black) and the negative charge in molecule (blue), respectively. (b) The level diagram for inelastic electron scattering mechanism at negative bias. The black lines denote the vacuum level at two electrodes, and the red lines represent the initial and final electronic states. $\mu_t \equiv \mu_0 + eV_b$ and $\mu_s \equiv \mu_0$ are the Fermi energies of tip and substrate at bias voltage V_b , where μ_0 is the Fermi energy of tip and substrate at zero bias.

of the single-molecule STML in Fig. 1(a). A molecule, simplified for clarity as a dipole with positive (red) and negative (blue) charge, is deposited on a salt-covered metal substrate. A metal tip is positioned above the substrate plane. Both the tip and substrate are typically used with noble metal, e.g., silver (Ag). With nonzero bias voltage, an electron (black) from one electrode excites the molecule via the Coulomb interaction during its tunneling through the vacuum and then enters into the other electrode (see Fig. 1(b)). Subsequently, the excited molecule emits a photon by the spontaneous emission, which is measured by the photon counting to reveal molecular properties.

The Hamiltonian for the setup is divided into three parts as $H = H_{el} + H_m + H_{el-m}$, where H_{el} is the Hamiltonian for the tunneling electron between the tip and substrate, H_m is the Hamiltonian of the molecule, and H_{el-m} is the interaction between the tunneling electron and the single molecule. The Hamiltonian of the tunneling electron is $H_{el} = -\nabla^2 / (2m_e) +$

$V(\mathbf{r})$, where $V(\mathbf{r})$ is the potential for the tunneling electron at position $\mathbf{r} = (x, y, z)$ and m_e is the mass of an electron. The wave functions are written for different regions [16, 17] as

$$H_{\text{el,t}}|\phi_k\rangle \simeq \tilde{\xi}_k|\phi_k\rangle, \quad (1a)$$

$$H_{\text{el,s}}|\varphi_n\rangle \simeq \tilde{E}_n|\varphi_n\rangle, \quad (1b)$$

where $H_{\text{el,t}}$ ($H_{\text{el,s}}$) is the Hamiltonian of the free tip (substrate) obtained by neglecting the potential in the substrate (tip) region. $|\phi_k\rangle$ ($|\varphi_n\rangle$) is the eigenstate of free tip (substrate) with $\tilde{\xi}_k \equiv \xi_k + eV_b$ ($\tilde{E}_n \equiv E_n$) where ξ_k (E_n) is the eigenenergy with zero bias voltage. The detailed form of the wave functions are discussed in the supplementary material. The Hamiltonian for the molecule is simplified as a two-level system [18, 19] $H_m = E_e|\chi_e\rangle\langle\chi_e| + E_g|\chi_g\rangle\langle\chi_g|$, where $|\chi_e\rangle$ ($|\chi_g\rangle$) is its excited (ground) state with energy E_e (E_g).

The key element to understand the mechanism is the interaction between the molecule and the tunneling electron. For the purpose of clarity, we consider a simple case of one tunneling electron. The interaction, simplified from the Coulomb interaction, resembles the dipole interaction as

$$H_{\text{el-m}} \simeq -e\frac{\vec{\mu} \cdot \vec{r}}{|\vec{r}|^3}, \quad (2)$$

where $\vec{\mu} = -Ze\vec{r}_0$ denotes the effective electric dipole moment of the molecule. Z is the effective charge number, and \vec{r}_0 stands for the vector of the center of the electrons in molecule. \vec{r} represents the vector of the tunneling electron. Here, we have chosen the central position of the positive charge of molecule as the origin of the coordinate system. The detailed

derivation can be found for the molecule with multiple chemical bonds [20] in the supplementary material.

The interaction is rewritten explicitly with the basis of the wave functions of the single molecule and tunneling electron as

$$\begin{aligned} H_{\text{el-m}} &= \sum_{n,k} \mathcal{N}_{\text{s,t}}|_{V_b, E_n \rightarrow \xi_k} \sigma_x |\phi_k\rangle \langle \varphi_n| \\ &= \sum_{n,k} \mathcal{N}_{\text{t,s}}|_{V_b, \xi_k \rightarrow E_n} \sigma_x |\varphi_n\rangle \langle \phi_k|. \end{aligned} \quad (3)$$

We have defined the transition matrix element $\mathcal{N}_{\text{s,t}}|_{V_b, E_n \rightarrow \xi_k} \equiv -e\vec{\mu} \cdot \langle \phi_k | \vec{r} / |\vec{r}|^3 | \varphi_n \rangle$ from substrate's state $|\varphi_n\rangle$ to tip's state $|\phi_k\rangle$ and $\mathcal{N}_{\text{t,s}}|_{V_b, \xi_k \rightarrow E_n} \equiv -e\vec{\mu} \cdot \langle \varphi_n | \vec{r} / |\vec{r}|^3 | \phi_k \rangle$ from tip's state $|\phi_k\rangle$ to substrate's state $|\varphi_n\rangle$. $\sigma_x \equiv |\chi_e\rangle\langle\chi_g| + |\chi_g\rangle\langle\chi_e|$ is the transition matrix between molecular ground and excited states. The electron-dipole interaction in Eq. (3) will induce energy transfer between the tunneling electron and the molecule (the state of the two-level molecule is flipped).

Tip's wave function in the vacuum region has the asymptotic spherical form $\phi_k(\mathbf{r}) = A_k e^{-\kappa_k |\mathbf{r} - \vec{a}|} / (\kappa_k |\mathbf{r} - \vec{a}|)$ where \vec{a} is the position of tip's center of curvature and $\kappa_k = \sqrt{-2m_e \xi_k}$ is its decay factor. The normalized coefficient A_k can be determined by first-principles calculations. This wave function is typical known as the s-wave, which is the simplest case for the tip [16, 21]. Contribution from other wave functions can be similarly considered as that in the studies of STM [21]. And substrate's wave function $\varphi_n(\mathbf{r}) = B_n e^{-\kappa_n |z|}$ decays along the $+z$ direction with decay factor $\kappa_n = \sqrt{-2m_e E_n}$ [22, 23] and the normalization constant B_n . With the wave functions for the tip and substrate, the transition matrix element is explicitly written as

$$\mathcal{N}_{\text{s,t}}|_{V_b, E_n \rightarrow \xi_k} \simeq -A_k B_n \sum_{l=x,y,z} e\mu_l \int_{-\infty}^{\infty} dx \int_{-\infty}^{\infty} dy \int_0^d dz l \frac{e^{-\kappa_n z - \kappa_k \sqrt{(x-a_x)^2 + y^2 + (z-d-R)^2}}}{(x^2 + y^2 + z^2)^{3/2}}, \quad (4)$$

where $\mu_{x(y,z)}$ is the $x(y,z)$ component of the molecular dipole moment. And without loss of generality, we have chosen the position of tip's center of curvature along x axis, i.e., $\vec{a} = (a_x, 0, d+R)$. By taking the decay wave functions of tip and substrate into account, we integrate over the region between plane $z=0$ and $z=d$ as an approximation. And in the later discussion, we ignore the dependence of $\mathcal{N}_{\text{s,t}}|_{V_b, E_n \rightarrow \xi_k}$ on the normalization constants A_k and B_n by taking them to independent on the index k and n .

Asymmetry of photon counting – To understand the asymmetry of photon counting, we calculate the tunneling rate at negative bias ($V_b < 0$), illustrated in Fig. 1(b), where the Fermi level of tip is lower than that of substrate. The molecule is initially in its ground state and the tunneling electron in one of

substrate's eigenstate, i.e., $|\Psi(t=0)\rangle = |\chi_g\rangle|\varphi_n\rangle$. To the first order of $H_{\text{el}} - H_{\text{el,s}}$ and $H_{\text{el-m}}$, we obtain the time evolution of the system as

$$\begin{aligned} |\Psi(t)\rangle &= e^{-i(\tilde{E}_n + E_g)t} |\chi_g\rangle|\varphi_n\rangle \\ &+ \sum_k c_{g,k}(t) |\chi_g\rangle|\phi_k\rangle + \sum_k c_{e,k}(t) |\chi_e\rangle|\phi_k\rangle, \end{aligned} \quad (5)$$

where the second and third terms stand for elastic and inelastic tunneling respectively. In order to obtain the above result, we have applied the rotating-wave approximation for Hamiltonian in Eq. (3). The corresponding tunneling amplitudes read

$$c_{g,k}(t) = e^{-iE_g t} \frac{e^{-i\tilde{E}_n t} - e^{-i\tilde{\xi}_k t}}{\tilde{E}_n - \tilde{\xi}_k} \mathcal{M}_{n,k}, \quad (6)$$

$$c_{e,k}(t) = \frac{e^{-i(\tilde{E}_n + E_g)t} - e^{-i(\tilde{\xi}_k + E_e)t}}{\tilde{E}_n - \tilde{\xi}_k - E_{eg}} \mathcal{N}_{s,t}|_{V_b, E_n \rightarrow \xi_k}, \quad (7)$$

where $\mathcal{M}_{n,k} \equiv \langle \phi_k | (H_{el} - H_{el,s}) | \phi_n \rangle$ is the transition matrix element of the elastic tunneling and $E_{eg} \equiv E_e - E_g$ is the optical gap of the single molecule.

We will focus on the inelastic tunneling process instead of the elastic tunneling which has been well explored in the earlier development [16, 21–23] of STM. The inelastic tunneling rate $\mathcal{J}_{n \rightarrow k}$ from $|\phi_n\rangle$ to $|\phi_k\rangle$ is $\mathcal{J}_{n \rightarrow k} = d|c_{e,k}(t)|^2/dt$. The overall inelastic electron current at negative voltage $I_{-,inela} = e \sum_n \sum_k \mathcal{J}_{n \rightarrow k} F_{\mu_0,T}(E_n) (1 - F_{\mu_0,T}(\xi_k))$ is explicitly rewritten as

$$I_{-,inela} = 2\pi e \int dE_n \rho_s(E_n) \rho_t(\xi_k) F_{\mu_0,T}(E_n) \times (1 - F_{\mu_0,T}(\xi_k)) |\mathcal{N}_{s,t}|_{V_b, E_n \rightarrow \xi_k}|^2_{\xi_k = E_n - eV_b - E_{eg}}, \quad (8)$$

where $\rho_t(E)$ ($\rho_s(E)$) are the density of state of tip (substrate) at the energy E . $F_{\mu_0,T}(E)$ is the Fermi-Dirac distribution of electrons in tip or substrate state at energy E , chemical potential μ_0 , and temperature T . $|\mathcal{N}_{s,t}|_{V_b, E_n \rightarrow \xi_k}|^2_{\xi_k = E_n - eV_b - E_{eg}}$ rules out all the tunneling processes whose energy do not conserve. Without loss of generality, we consider here the tip and substrate are of the same metal (Ag).

In STML experiment, the temperature of the ultrahigh-vacuum chamber is low enough, typically lower than 10K [6–13, 24, 25], that the Fermi-Dirac distribution function is approximately a Heaviside function, i.e., $F_{\mu_0,T}(E) = 1$ for $E < \mu_0$ and $F_{\mu_0,T}(E) = 0$ for $E > \mu_0$. The inelastic tunneling current becomes

$$I_{-,inela} \simeq 2\pi e \int_{\mu_0 + eV_b + E_{eg}}^{\mu_0} dE_n \rho_s(E_n) \rho_t(\xi_k) \times |\mathcal{N}_{s,t}|_{V_b, E_n \rightarrow \xi_k}|^2_{\xi_k = E_n - eV_b - E_{eg}} \quad (9)$$

Eq. (9) suggests that the current for inelastic tunneling is nonzero only at the condition $eV_b < -E_{eg}$ for the negative bias case.

For the positive bias $V_b > 0$, the current for the inelastic tunneling is obtained with the similar method as

$$I_{+,inela} \simeq 2\pi e \int_{\mu_0}^{\mu_0 + eV_b - E_{eg}} dE_n \rho_s(E_n) \rho_t(\xi_k) \times |\mathcal{N}_{s,t}|_{V_b, \xi_k \rightarrow E_n}|^2_{\xi_k = E_n - eV_b + E_{eg}}. \quad (10)$$

Similar to the negative bias case, the condition for a nonzero inelastic current is $eV_b > E_{eg}$. The equal bias voltage for nonzero inelastic current at negative and positive bias is an

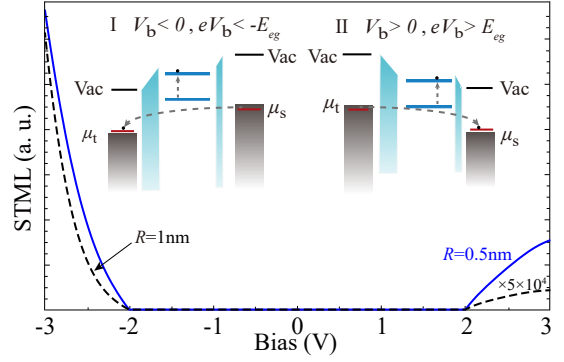


Figure 2. Asymmetric photon intensity in inelastic electron scattering mechanism. The blue solid (black dashed) line represents the emission intensity for tip's center of curvature $R = 0.5$ (1) nm. Two insets show the inelastic electron scattering mechanism for a two-level molecule at the negative and positive bias. The molecular optical gap is $E_{eg} = 2$ eV, and the Fermi energy of silver is $\mu_0 = -4.64$ eV. The distance between tip and molecule is $d = 0.4$ nm. Here, we choose the case where the tip is deposited right above the molecule and the molecular transition dipole is along the z axis.

important feature different from the carrier-injection mechanism where the electron injection requires different voltage for the negative and positive bias [6, 26]. With Eqs. (9 and 10), we obtain the inelastic tunneling current as

$$I_{inela} = \begin{cases} I_{-,inela}, & V_b < -\frac{E_{eg}}{e} \\ 0, & -\frac{E_{eg}}{e} \leq V_b \leq \frac{E_{eg}}{e} \\ I_{+,inela}, & V_b > \frac{E_{eg}}{e} \end{cases}. \quad (11)$$

Photon counting of molecular fluorescence is a quantity relevant for probing the properties of the single molecule. Once excited, the molecule will decay to its lower state spontaneously with rate γ . The photon counting rate is proportional to the inelastic current

$$\Gamma = I_{inela}/e. \quad (12)$$

The detailed derivation can be found in the supplementary materials. In Fig. 2, we plot the photon counting rate as the function of the bias voltage between the tip and the substrate. The blue solid and black dashed lines show the relative emission intensity for tip's center of curvature $R = 0.5$ nm and 1 nm, respectively. The Fermi energy of silver is $\mu_0 = -4.64$ eV, and the density of state of silver can be found in [27]. Without loss of generality, we choose the tip right above the molecule ($a_x = 0$) and the molecular dipole along the z direction ($\mu_z \neq 0$ while $\mu_x = \mu_y = 0$). The distance between tip and molecule is $d = 0.4$ nm. As predicted in Eq. (11), the bias voltages for nonzero inelastic current at negative and positive bias are the same, i.e., $|eV_b| > E_{eg} = 2$ eV. Insets in Fig. 2 describe the mechanism of the inelastic electron scattering.

Another important feature is the asymmetry of the larger photon counting at negative bias than that at positive bias, as illustrated in Fig. 2. This intensity asymmetry stems from

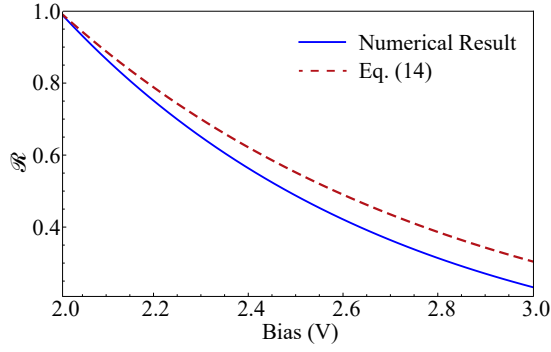


Figure 3. The ratio \mathcal{R} between the photon counting at the positive and negative voltages. The solid line shows the ratio calculated with the exact tunneling rate from Eqs. (9 and 10), and the dashed line shows the analytical formula for the ratio in Eq. (14).

the eigenfunction asymmetry of tip and substrate. The tip's wave function $\phi_k(\vec{r})$ decays spherically with factor κ_k , and substrate's wave function $\phi_n(\vec{r})$ decays along the $+z$ direction with factor κ_n . The relation between the elements of the transition matrix at positive bias V_b and that at negative bias $-V_b$ reads

$$\mathcal{N}_{t,s}|_{V_b, \xi_k \rightarrow E_n} \simeq e^{-(\kappa_k - \kappa_n)R} \mathcal{N}_{s,t}|_{-V_b, \xi_k \rightarrow E_n}. \quad (13)$$

The ratio between the transition matrix element at positive bias V_b and that at negative bias $-V_b$ is $e^{-(\kappa_k - \kappa_n)R}$. Inserting Eq. (13) into Eq. (9), we obtain the ratio of the emission intensity as (see Supplementary Material for details)

$$\mathcal{R} = \frac{I_{+, \text{inela}}|_{V_b}}{I_{-, \text{inela}}|_{-V_b}} \simeq e^{-R\sqrt{-2m_e\mu_0} \frac{eV_b - E_{eg}}{-\mu_0}} < 1. \quad (14)$$

The current equation shows the characteristic asymmetry with larger current at negative bias induced by inelastic electron tunneling. Such asymmetry for inelastic scattering is caused by geometry shape of the tip and the substrate, and persists with different materials.

In Fig. 3, we show the dependence of the asymmetrical ratio \mathcal{R} as a function of the bias voltage with both the analytical formula (red dashed line) in Eq. (14) and the numerical result (blue solid line) calculated with the exact tunneling rate from Eqs. (9-10). The analytical formula shows an agreement on the trend that the asymmetry of the photon counting increases with increasing bias voltage. The exponential decay of the ratio \mathcal{R} as function of bias voltage is predicted in Eq. (14) and shall be tested with the experimental data.

With the theoretical predictions above, we revisit the important features observed in recent experiments [6, 12, 13]. In the single-hydrocarbon fluorescence induced by STM [12], the phenomenon that the emission intensity at positive bias was lower than that at negative bias is in line with our prediction. Though such the asymmetric intensity feature (the intensity at positive bias was much lower than that at negative bias) of a single ZnPc molecule was attributed to the carrier-injection

mechanism [6], we emphasize that the inelastic electron scattering mechanism may also play an important role in this feature. By changing the tip and substrate material from Ag to Au, Doppagne *et al.* [13] observed a phenomenon which was opposite to the feature in [6]. The emission of a single neutral ZnPc molecule at positive bias was 30 times more intense than that at negative bias. Our theory definitely excludes the inelastic electron scattering mechanism as the origin of such asymmetric luminescence in [13].

In conclusion, we have derived the microscopic origin of the molecular excitation via the inelastic electron scattering mechanism in single-molecule STML. By the model, we obtain the emission intensity in the inelastic electron scattering mechanism. We find that inelastic electron scattering mechanism requires a symmetric bias voltage for nonzero inelastic current which equals the optical gap of this two-level molecule exactly. It implies that the energy window between the Fermi levels of two electrodes should at least equal the optical gap of the molecule [26]. Importantly, we reveal an asymmetric emission intensity at negative and positive bias which is due to the asymmetric forms of wave functions at two electrodes and show that the ratio of such asymmetry decays with tip's radius of curvature and bias voltage. Our model offers us a theoretical insight into the molecular excitation in the inelastic electron scattering process which has never been explored before.

Before closing, it is worthy to mention that the inelastic scattering mechanism is one of the three mechanisms proposed now and the photon counting obtained here is one part of the total emission intensity. Further research is needed for elucidating the competition of these three mechanisms and finding the dominant one under certain conditions.

H. D. thanks Yang Zhang for the helpful discussion. This work is supported by the NSFC (Grants No. 11534002 and No. 11875049), the NSAF (Grant No. U1730449 and No. U1530401), and the National Basic Research Program of China (Grants No. 2016YFA0301201 and No. 2014CB921403). H.D. also thanks The Recruitment Program of Global Youth Experts of China.

* hdong@gscaep.ac.cn

- [1] S. V. Aradhya and L. Venkataraman, *Nat. Nanotechnol.* **8**, 399 (2013).
- [2] N. Xin, J. Guan, C. Zhou, X. Chen, C. Gu, Y. Li, M. A. Ratner, A. Nitzan, J. F. Stoddart, and X. Guo, *Nat. Rev. Phys.* **1**, 211 (2019).
- [3] L. L. Sun, Y. A. Diaz-Fernandez, T. A. Gschneidner, F. Westerglund, S. Lara-Avila, and K. Moth-Poulsen, *Chem. Soc. Rev.* **43**, 7378 (2014).
- [4] E. Flaxer, O. Sneh, and O. Cheshnovsky, *Science* **262**, 2012 (1993).
- [5] R. Berndt, R. Gaisch, J. K. Gimzewski, B. Reihl, R. R. Schlittler, W. D. Schneider, and M. Tschudy, *Science* **262**, 1425 (1993).
- [6] Y. Zhang, Y. Luo, Y. Zhang, Y. J. Yu, Y. M. Kuang, L. Zhang,

- Q. S. Meng, Y. Luo, J. L. Yang, Z. C. Dong, and J. G. Hou, *Nature (London)* **531**, 623 (2016).
- [7] B. Doppagne, M. C. Chong, E. Lorchat, S. Berciaud, M. Romeo, H. Bulou, A. Boeglin, F. Scheurer, and G. Schull, *Phys. Rev. Lett.* **118**, 127401 (2017).
- [8] Y. Luo, G. Chen, Y. Zhang, L. Zhang, Y. J. Yu, F. F. Kong, X. J. Tian, Y. Zhang, C. X. Shan, Y. Luo, J. L. Yang, V. Sandogh-dar, Z. C. Dong, and J. G. Hou, *Phys. Rev. Lett.* **122**, 233901 (2019).
- [9] H. Imada, K. Miwa, M. Imai-Imada, S. Kawahara, K. Kimura, and Y. Kim, *Nature (London)* **538**, 364 (2016).
- [10] H. Imada, K. Miwa, M. Imai-Imada, S. Kawahara, K. Kimura, and Y. Kim, *Phys. Rev. Lett.* **119**, 013901 (2017).
- [11] Y. Zhang, Q. S. Meng, L. Zhang, Y. Luo, Y. J. Yu, B. Yang, Y. Zhang, R. Esteban, J. Aizpurua, Y. Luo, J. L. Yang, Z. C. Dong, and J. G. Hou, *Nat. Commun.* **8**, 15225 (2017).
- [12] J. Kröger, B. Doppagne, F. Scheurer, and G. Schull, *Nano Lett.* **18**, 3407 (2018).
- [13] B. Doppagne, M. C. Chong, H. Bulou, A. Boeglin, F. Scheurer, and G. Schull, *Science* **361**, 251 (2018).
- [14] X. Y. Wu, R. L. Wang, Y. Zhang, B. W. Song, and C. Y. Yam, *J. Phys. Chem. C* **123**, 15761 (2019).
- [15] K. Miwa, H. Imada, M. Imai-Imada, K. Kimura, M. Galperin, and Y. Kim, *Nano Lett.* **19**, 2803 (2019).
- [16] J. Bardeen, *Phys. Rev. Lett.* **6**, 57 (1961).
- [17] A. D. Gottlieb and L. Wesoloski, *Nanotechnology* **17**, R57 (2006).
- [18] L. L. Nian, Y. Wang, and J. T. Lü, *Nano Lett.* **18**, 6826 (2018).
- [19] L. L. Nian and J. T. Lü, *J. Phys. Chem. C* **123**, 18508 (2019).
- [20] V. I. Minkin, O. A. Osipov, and Y. A. Zhdanov, *DIPOLE MOMENTS IN ORGANIC CHEMISTRY*, 1st ed., edited by W. E. Vaughan (Plenum Press, New York, 1970) pp. 79.
- [21] C. J. Chen, *Phys. Rev. B* **42**, 8841 (1990).
- [22] J. Tersoff and D. R. Hamann, *Phys. Rev. Lett.* **50**, 1998 (1983).
- [23] J. Tersoff and D. R. Hamann, *Phys. Rev. B* **31**, 805 (1985).
- [24] G. Chen, Y. Luo, H. Y. Gao, J. Jiang, Y. J. Yu, L. Zhang, Y. Zhang, X. G. Li, Z. Y. Zhang, and Z. C. Dong, *Phys. Rev. Lett.* **122**, 177401 (2019).
- [25] K. Miwa, H. Imada, M. Imai-Imada, S. Kawahara, J. Takeya, M. Kawai, M. Galperin, and Y. Kim, *Nature (London)* **570**, 210 (2019).
- [26] M. C. Chong, *Electrically driven fluorescence of single molecule junctions*, *Ph.D. thesis*, Université de Strasbourg, France (2016).
- [27] D. A. Papaconstantopoulos, *Handbook of the band structure of elemental solids: from Z = 1 to Z = 112*, 2nd ed. (Springer, New York, 2015) pp. 243.

Microscopic origin of molecule excitation via inelastic electron scattering in scanning tunneling microscope

Guohui Dong,¹ Yining You,² and Hui Dong^{1,*}

¹Graduate School of Chinese Academy of Engineering Physics, Beijing 100084, China

²Department of Modern Physics, University of Science and Technology of China, Hefei 230026, China

This document is devoted to providing the detailed derivations and the supporting discussions to the main content.

I. ELECTRONIC WAVE FUNCTIONS ON THE TIP AND SUBSTRATE

In this section, we show the details to the wave function of the tunneling electron Hamiltonian,

$$H_{\text{el}} = -\frac{1}{2m_e}\nabla^2 + V(\mathbf{r}). \quad (1)$$

The total potential $V(\mathbf{r})$, illustrated in Fig. 1(a), is divided into two parts: the tip $V_t(\mathbf{r})$ (subfigure (b)), and the substrate part $V_s(\mathbf{r})$ (subfigure (c)). We use the approximate method proposed by Bardeen in 1961 [1, 2]. The Hamiltonian of the free tip and substrate, $H_{\text{el,t}} = -\nabla^2/2m_e + V_t(\mathbf{r})$ and $H_{\text{el,s}} = -\nabla^2/2m_e + V_s(\mathbf{r})$. For zero bias $V_b = 0$, the eigenstates of the free tip and substrate are

$$H_{\text{el,t}}|_{V_b=0}|\phi_k\rangle = \xi_k|\phi_k\rangle, \quad (2a)$$

$$H_{\text{el,s}}|_{V_b=0}|\varphi_n\rangle = E_n|\varphi_n\rangle, \quad (2b)$$

where $H_{\text{el,t(s)}}|_{V_b=0}$ represents the free tip (substrate) Hamiltonian at zero bias and $|\phi_k\rangle(|\varphi_n\rangle)$ is the eigenstate of free tip (substrate) with energy $\xi_k(E_n)$. As the tip apex has been modeled as a metal sphere, its wave function in the vacuum region has the asymptotic spherical form

$$\phi_k(\mathbf{r}) = A_k \frac{e^{-\kappa_k|\mathbf{r}-\mathbf{a}|}}{\kappa_k|\mathbf{r}-\mathbf{a}|}, \quad (3)$$

where \mathbf{a} is the tip's center of curvature and $\kappa_k = \sqrt{-2m_e\xi_k}$ is its decay factor. A_k can be determined by the first-principles calculations. On the other hand, in the vacuum region, we take substrate's wave function as

$$\varphi_n(\mathbf{r} \equiv (x, y, z)) = B_n e^{-\kappa_n|z|}, \quad (4)$$

where $\kappa_n = \sqrt{-2m_eE_n}$ is the decay factor.

For nonzero bias $V_b \neq 0$, we take the potential change induced by bias voltage as a perturbation and obtain the solution up to the first-order correction,

$$H_{\text{el,t}}|\phi_k\rangle \simeq \tilde{\xi}_k|\phi_k\rangle, \quad (5a)$$

$$H_{\text{el,s}}|\varphi_n\rangle \simeq \tilde{E}_n|\varphi_n\rangle, \quad (5b)$$

where $H_{\text{el,t(s)}}$ represents the free tip (substrate) Hamiltonian at bias V_b and $\tilde{\xi}_k \equiv \xi_k + eV_b$ ($\tilde{E}_n \equiv E_n$) is the corrected energy of state $|\phi_k\rangle(|\varphi_n\rangle)$. Here we neglect the change to the wave function of the tip induced by the applied voltage [3].

II. THE ELECTRON-MOLECULE INTERACTION

In this section, we show the detailed derivation of the the effective electron-dipole interaction between a tunneling electron and a single molecule. The Coulomb interaction between a tunneling electron and the molecule is written as

$$H_{\text{el-m}} = \sum_{n=1}^N \left(-\frac{Z_n e^2}{|\mathbf{r} - \mathbf{R}_n|} + \frac{Z_n e^2}{|\mathbf{r} - \mathbf{r}_n|} \right), \quad (6)$$

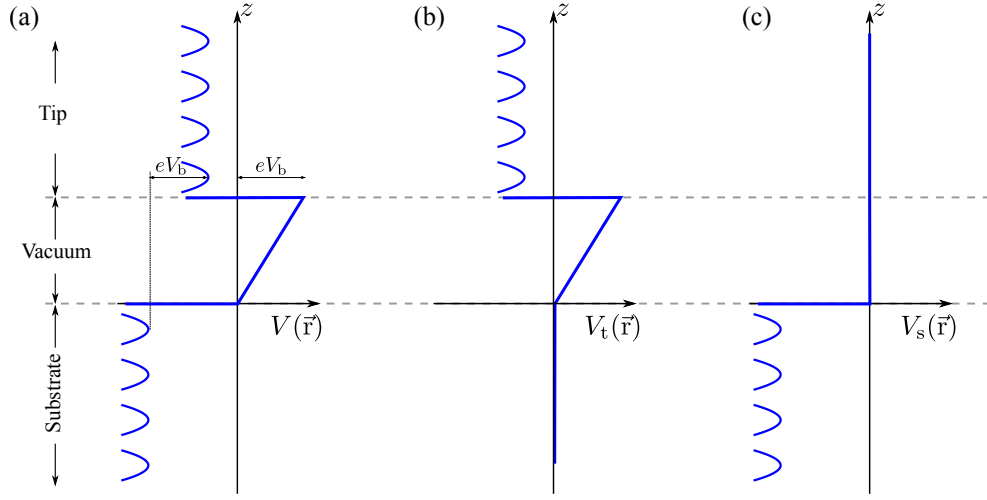


Figure 1. The schematic diagrams of the potential along z -axis. (a) The potential $V(\vec{r})$ of the tip and substrate. (b) The potential $V_t(\vec{r})$ for the tip. (c) The potential $V_s(\vec{r})$ for the substrate.

where \vec{r} is the position of the tunneling electron. The molecule contains N bonds. For the n -th bond, $\vec{R}_n(\vec{r}_n)$ is the position of positive (negative) charge with effective charge Z_n . $\vec{R}_0 \equiv \sum_{n=1}^N \vec{R}_n Z_n / \sum_{n=1}^N Z_n$ denotes the center of the positive charge. For the case where the distance between the tunneling electron and the molecule is much larger than the size of the molecule, i.e., $|\vec{r} - \vec{R}_0| \gg |\vec{R}_n - \vec{R}_0|, |\vec{r}_n - \vec{R}_0|$ for all n , the coupling in Eq. (6) becomes

$$\begin{aligned}
H_{\text{el-m}} &= \sum_{n=1}^N \left(\frac{Z_n e^2}{|\vec{r} - \vec{r}_n|} - \frac{Z_n e^2}{|\vec{r} - \vec{R}_n|} \right) \\
&= \sum_{n=1}^N \left(\frac{Z_n e^2}{|\vec{r} - \vec{R}_0 + \vec{R}_0 - \vec{r}_n|} - \frac{Z_n e^2}{|\vec{r} - \vec{R}_0 + \vec{R}_0 - \vec{R}_n|} \right) \\
&= \sum_{n=1}^N \frac{Z_n e^2}{|\vec{r} - \vec{R}_0|} \left(\frac{1}{\left(1 + \frac{2(\vec{r} - \vec{R}_0) \cdot (\vec{R}_0 - \vec{r}_n)}{|\vec{r} - \vec{R}_0|^2} + \frac{|\vec{R}_0 - \vec{r}_n|^2}{|\vec{r} - \vec{R}_0|^2} \right)^{1/2}} - \frac{1}{\left(1 + \frac{2(\vec{r} - \vec{R}_0) \cdot (\vec{R}_0 - \vec{R}_n)}{|\vec{r} - \vec{R}_0|^2} + \frac{|\vec{R}_0 - \vec{R}_n|^2}{|\vec{r} - \vec{R}_0|^2} \right)^{1/2}} \right) \\
&\simeq \sum_{n=1}^N \frac{Z_n e^2}{|\vec{r} - \vec{R}_0|} \left(\left(1 - \frac{(\vec{r} - \vec{R}_0) \cdot (\vec{R}_0 - \vec{r}_n)}{|\vec{r} - \vec{R}_0|^2} \right) - \left(1 - \frac{(\vec{r} - \vec{R}_0) \cdot (\vec{R}_0 - \vec{R}_n)}{|\vec{r} - \vec{R}_0|^2} \right) \right) \\
&= \sum_{n=1}^N \frac{Z_n e^2}{|\vec{r} - \vec{R}_0|^3} (\vec{r} - \vec{R}_0) \cdot (\vec{r}_n - \vec{R}_n) \\
&= -e \frac{(\vec{r} - \vec{R}_0) \cdot \vec{\mu}}{|\vec{r} - \vec{R}_0|^3}, \tag{7}
\end{aligned}$$

where $\vec{\mu} = \sum_{n=1}^N Z_n e (\vec{R}_n - \vec{r}_n) = -Ze (\vec{R}_0 - \vec{r}_0)$, ($Z \equiv \sum_{n=1}^N Z_n, \vec{r}_0 \equiv \sum_{n=1}^N Z_n \vec{r}_n / Z$) denotes the total electric dipole moment of the molecule [4]. We set the position of the positive charge as the origin of the coordinate axes, i.e., $\vec{R}_0 = 0$. The electron-molecule interaction is expressed as

$$H_{\text{el-m}} \simeq -e \frac{\vec{r} \cdot \vec{\mu}}{|\vec{r}|^3}. \tag{8}$$

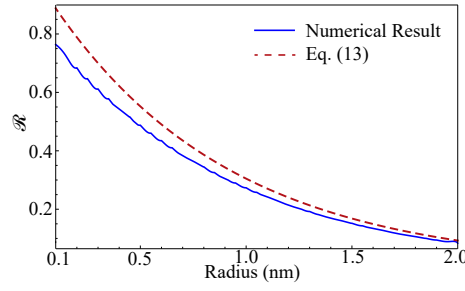


Figure 2. Photon intensity ratio versus the radius of tip. The blue solid line represents the result obtained by numerical calculation of the inelastic current and the red dashed line shows the result given in Eq. (13). Here, the positive bias is fixed to +2.5eV.

III. THE PHOTON COUNT RATE

Once excited to its excited state, the molecule will decay to its lower state and emits a photon spontaneously. Its photon counting rate is proportional to its probability in excited state, $p_e(t) \equiv \sum_{n,k} |c_{e,k}(t)|^2$. Taking the molecular excitation and the spontaneous emission process together, we obtain the master equation for this excitation probability

$$\frac{d}{dt} p_e(t) = -\gamma p_e(t) + \frac{I_{\text{inela}}}{e}, \quad (9)$$

where γ is the molecular spontaneous emission rate. In the steady state, the excitation probability becomes $p_e(t) = I_{\text{inela}}/e\gamma$. Then the photon counting rate becomes

$$\Gamma = \gamma \frac{I_{\text{inela}}}{e\gamma} = \frac{I_{\text{inela}}}{e}. \quad (10)$$

IV. THE RATIO OF EMISSION INTENSITY

$\varphi_n(\vec{\mathbf{r}})$ decays along the +z direction [5, 6]. At positive bias $V_b > 0$, the transition matrix element of the inelastic tunneling reads

$$\begin{aligned} \mathcal{N}_{t,s}|_{V_b, \xi_k \rightarrow E_n} &= \langle \phi_k | H_{e-m} | \varphi_n \rangle \\ &= -e\mu_z \langle \phi_k | \frac{z}{|\vec{\mathbf{r}}|^3} | \varphi_n \rangle \\ &= -2\pi A_k B_n e\mu_z \int_0^d dz \int_0^\infty dl \frac{e^{-\kappa_k \sqrt{x^2+y^2+(R+d-z)^2}}}{\kappa_k \sqrt{x^2+y^2+(R+d-z)^2}} \frac{z}{\sqrt{z^2+l^2}^3} e^{-\kappa_n z} \\ &\simeq -2\pi A_k B_n e\mu_z \int_0^d dz \int_0^\infty dl \frac{e^{-\kappa_k(R+d-z)}}{\kappa_k \sqrt{x^2+y^2+(R+d-z)^2}} \frac{z}{\sqrt{z^2+l^2}^3} e^{-\kappa_n z} \\ &= -2\pi A_k B_n e\mu_z e^{-(\kappa_k-\kappa_n)R} \int_0^d dz \int_0^\infty dl \frac{e^{-\kappa_n(R+d-z)}}{\kappa_k \sqrt{x^2+y^2+(R+z)^2}} \frac{d-z}{\sqrt{(d-z)^2+l^2}^3} e^{-\kappa_k z} \\ &\simeq e^{-(\kappa_k-\kappa_n)R} \mathcal{N}_{s,t}|_{-V_b, \xi_k \rightarrow E_n}, \end{aligned} \quad (11)$$

where $\mathcal{N}_{t,s}|_{V_b, \xi_k \rightarrow E_n}$ is the transition matrix element of the inelastic tunneling from tip's state $\phi(\vec{\mathbf{r}})$ with energy $\xi_k + eV_b$ to substrate's state $\varphi(\vec{\mathbf{r}})$ with energy E_n at bias V_b and $\mathcal{N}_{s,t}|_{-V_b, \xi_k \rightarrow E_n}$ is the transition matrix element of the inelastic tunneling from substrate's state $\varphi(\vec{\mathbf{r}})$ with energy ξ_k to tip's state $\phi(\vec{\mathbf{r}})$ with energy $E_n - e|V_b|$. Without loss of generality, we have chosen the tip right above the molecule ($|OA| = 0$) and the molecular dipole in the z direction ($\mu_z \neq 0$ while $\mu_x = \mu_y = 0$). In deriving Eq. (11), we have taken the approximation that, in the vacuum region, tip's state only decays in z direction. We see that for the same initial energy, the ratio of the transition matrix element at positive bias V_b to that at negative bias $-V_b$ is $e^{-(\kappa_k-\kappa_n)R}$. Then, the

inelastic tunneling current at positive bias is

$$\begin{aligned}
I_{+, \text{inela}}|_{V_b} &\simeq 2\pi e \int_{\mu_0}^{\mu_0 + eV_b - E_{eg}} dE_n \rho_s(E_n) \rho_t(\xi_k) \left| \mathcal{N}_{s,t}|_{V_b, \xi_k \rightarrow E_n} \right|^2 \Big|_{\xi_k = E_n - eV_b + E_{eg}} \mathbb{R} \\
&\simeq 2\pi e \int_{\mu_0}^{\mu_0 + eV_b - E_{eg}} dE_n e^{-2\sqrt{-2m_e E_n} \left(\sqrt{1 - \frac{eV_b - E_{eg}}{E_n}} - 1 \right) R} \rho_s(E_n) \rho_t(\xi_k) \left| \mathcal{N}_{s,t}|_{-V_b, \xi_k \rightarrow E_n} \right|^2 \Big|_{\xi_k = E_n - eV_b + E_{eg}}, \quad (12)
\end{aligned}$$

where $\rho_t(E)$ ($\rho_s(E)$) denotes the density of state of tip (substrate) at the energy E and μ_0 is the Fermi energy of substrate and tip at zero bias. For a small bias which satisfies $(eV_b - E_{eg})/\mu_0 \ll 1$, Eq. (12) can be further simplified as

$$\begin{aligned}
I_{+, \text{inela}}|_{V_b} &\simeq 2\pi e \int_{\mu_0}^{\mu_0 + eV_b - E_{eg}} dE_n e^{\sqrt{-2m_e E_n} \left(\frac{eV_b - E_{eg}}{E_n} \right) R} \rho_s(E_n) \rho_t(\xi_k) \left| \mathcal{N}_{s,t}|_{-V_b, \xi_k \rightarrow E_n} \right|^2 \Big|_{\xi_k = E_n - eV_b + E_{eg}} \\
&\simeq e^{-R\sqrt{-2m_e \mu_0} \left(\frac{eV_b - E_{eg}}{-\mu_0} \right)} 2\pi e \rho_s(\mu_0) \rho_t(\mu_0) \int_{\mu_0}^{\mu_0 + eV_b - E_{eg}} dE_n \left| \mathcal{N}_{s,t}|_{-V_b, \xi_k \rightarrow E_n} \right|^2 \Big|_{\xi_k = E_n - eV_b + E_{eg}} \\
&\simeq e^{-R\sqrt{-2m_e \mu_0} \left(\frac{eV_b - E_{eg}}{-\mu_0} \right)} I_{-, \text{inela}}|_{-V_b}. \quad (13)
\end{aligned}$$

For noble metal, such as Au, Ag, and Cu, its density of state is almost a constant for several electron volt around its Fermi energy [7]. Thus, in deriving Eq. (13), we have extracted the density of state function from the integral. Finally, we see in Eq. (13) that this ratio decays with tip's radius R and bias voltage V_b .

Fig. 2 shows the ratio $I_{+, \text{inela}}|_{V_b}/I_{-, \text{inela}}|_{-V_b}$ with bias and tip's radius of curvature. The blue line represents the numerical result and the red line shows the analytical result presented in Eq.(15) of the main context. Fig. 2 shows that the ratio decays with the increase of tip's radius. And the larger the radius is, the better the two results coincide with each other. The underlying reason is that the main contribution of the integral in the transition matrix element comes from a small region between the tip and the molecule. And in deriving Eq. (13), we also have taken the approximation that, in the vacuum, tip's wave only decays in z direction. Thus, for a tip with a larger radius, tip's wave function behaves more like a wave that decays only in z direction in the small region under tip.

* hdong@gscaep.ac.cn

- [1] J. Bardeen, *Phys. Rev. Lett.* **6**, 57 (1961).
- [2] A. D. Gottlieb and L. Wesoloski, *Nanotechnology* **17**, R57 (2006).
- [3] C. J. Chen, *Phys. Rev. B* **42**, 8841 (1990).
- [4] V. I. Minkin, O. A. Osipov, and Y. A. Zhdanov, *DIPOLE MOMENTS IN ORGANIC CHEMISTRY*, 1st ed., edited by W. E. Vaughan (Plenum Press, New York, 1970) pp. 79.
- [5] J. Tersoff and D. R. Hamann, *Phys. Rev. Lett.* **50**, 1998 (1983).
- [6] J. Tersoff and D. R. Hamann, *Phys. Rev. B* **31**, 805 (1985).
- [7] D. A. Papaconstantopoulos, *Handbook of the band structure of elemental solids: from Z = 1 to Z = 112*, 2nd ed. (Springer, New York, 2015) pp. 243.